Communicated by Wilfrid Rall

The Impact of Parallel Fiber Background Activity on the Cable Properties of Cerebellar Purkinje Cells

Moshe Rapp
Yosef Yarom
Idan Segev
Department of Neurobiology, Institute of Life Sciences, The Hebrew University, Jerusalem, 91904, Israel

Neurons in the mammalian CNS receive 10^4–10^5 synaptic inputs onto their dendritic tree. Each of these inputs may fire spontaneously at a rate of a few spikes per second. Consequently, the cell is bombarded by several hundred synapses in each and every millisecond. An extreme example is the cerebellar Purkinje cell (PC) receiving approximately 100,000 excitatory synapses from the parallel fibers (p.f.s) onto dendritic spines covering the thin dendritic branchlets. What is the effect of the p.f.s activity on the integrative capabilities of the PC? This question is explored theoretically using analytical cable models as well as compartmental models of a morphologically and physiologically characterized PC from the guinea pig cerebellum. The input of individual p.f.s was modeled as a transient conductance change, peaking at 0.4 nS with a rise time of 0.3 msec and a reversal potential of +60 mV relative to rest. We found that already at a firing frequency of a few spikes per second the membrane conductance is several times larger than the membrane conductance in the absence of synaptic activity. As a result, the cable properties of the PC significantly change; the most sensitive parameters are the system time constant (τ_0) and the steady-state attenuation factor from dendritic terminal to soma. The implication is that the cable properties of central neurons in freely behaving animals are different from those measured in slice preparation or in anesthetized animals, where most of the synaptic inputs are inactive. We conclude that, because of the large conductance increase produced by the background activity of the p.f.s, the activity of the PC will be altered from this background level either when the p.f.s change their firing frequency for a period of several tens of milliseconds or when a large population of the p.f.s fires during a narrow time window.

1 Introduction

The processing of synaptic information by nerve cells is a function of the morphology and the electrical properties of the membrane and cytoplasm, as well as the site and properties of the synaptic inputs that impinge onto the dendritic tree. The theoretical studies of W. Rall (1959, 1964, 1967, 1977) have shown that in a passive tree the relevant parameters that determine this processing are the input resistance of the cell (R_N), the average electrotonic length of the dendrites (L_{AV}), the system time constant (τ_0), the rise time (t_{peak}) and magnitude (g_{max}) of the synaptic conductance change, as well as the reversal potential (E_{syn}) of the synaptic current. Rall's studies, followed by the study of Jack and Redman (1971a), suggested experimental methods for estimating these parameters. Consequently, several neuron types were characterized based on these parameters (e.g., Jack and Redman 1971b; Barrett and Crill 1974; Brown *et al.* 1981; Stratford *et al.* 1989; Nitzan *et al.* 1990). These studies were performed either on anesthetized animals or on slice preparations where most of the background synaptic activity is absent. However, neurons in the CNS are part of a large network and, therefore, each neuron receives thousands of synaptic inputs which may have ongoing activity of a few spikes per second. Such a massive input will generate a sustained conductance change which will modify the integrative capabilities of the neuron (Holmes and Woody 1989).

The present study explores the effect of this conductance change on the integrative properties of the cell, using detailed cable and compartmental models of a morphologically and physiologically characterized Purkinje cell (PC) from the guinea pig cerebellum (Rapp 1990; Segev *et al.* 1991). This cell has a large and complex dendritic tree (Fig. 1) with several hundred spiny branchlets (Fig. 2) that are densely studded with spines. Each of these spines receives an excitatory (asymmetrical) synaptic input from the parallel fiber (p.f.) system, summing to a total of $\sim 100,000$ p.f.s impinging on a single PC. In such a large system, even a low spontaneous activity rate of each of the p.f.s will generate a high frequency of synaptic input to the PC. The consequences of such an input for the input/output properties of the PC are discussed.

2 Model

Simulations were performed using cable and compartmental models of the cell shown in Figure 1. The cable properties of the same cell were estimated from intra-somatic recordings performed in the presence of 2.5 mM Cs^+ ions that abolish the marked subthreshold membrane rectification of these cells (Crapel and Penit-Soria 1986; Rapp 1990; Segev *et al.* 1991). The process of utilizing the model to estimate the specific membrane resistivity (R_m) and capacitance (C_m), and the specific

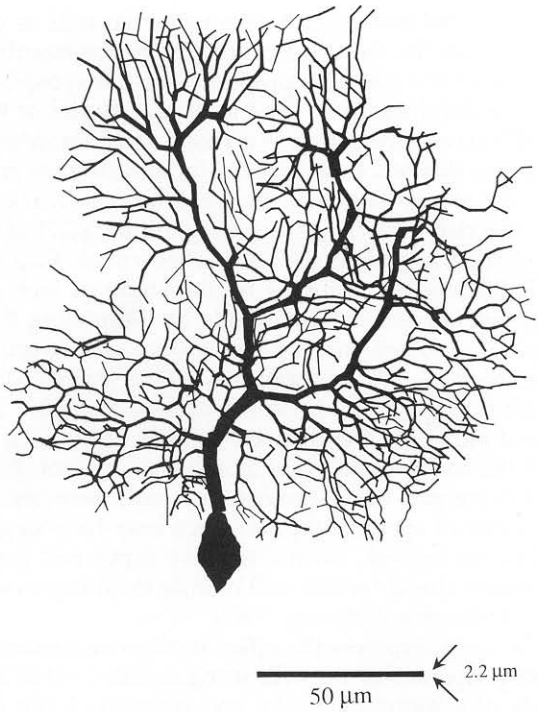

Figure 1: The modeled Purkinje cell. This cell was reconstructed following an intracellular injection of horseradish peroxidase. The cable parameters of the cell were also characterized in the presence of 2.5 mM Cs^+ ions to abolish the marked rectification that exists near the resting potential. The input resistance (R_N) was 12.9 MΩ and the system time constant (τ_0) was 46 msec. Assuming a total spine number of 100,000, each with an area of 1 μm^2, the soma-dendritic surface area sums to 149,500 μm^2. The optimal matching between the morphology and the cable properties of the cell implies that R_m is 440 $\Omega \cdot cm^2$ at the soma and 110,000 $\Omega \cdot cm^2$ at the dendrites, C_m is 1.64 $\mu F/cm^2$ and R_i is 250 $\Omega \cdot cm$.

Figure 2: *Facing page.* Sholl diagram, in morphological units, of the cell shown in Figure 1. This cell was represented by 1500 cylindrical segments and a spherical soma. Red lines denote the spiny branchlets that are studded with approximately 10 spines per 1 μm dendritic length. Each of these spines receives an excitatory input from a parallel fiber. These branchlets consist of 85% of the dendritic area (without the spines). The cell consists of 473 dendritic terminals, some of which terminate less than 100 μm away from the soma whereas others extend to a distance close to 400 μm from the soma. Because the parallel fibers impinge only on the spiny branchlets, these branchlets are electrically "stretched" when the parallel fibers are active.

resistivity of the cytoplasm (R_i) is elaborated in Segev *et al.* (1989) and Nitzan *et al.* (1990). For the PC under study the optimal match between the cell morphology and electrical measurements was obtained with R_m = 440 $\Omega \cdot cm^2$ at the soma and 110,000 $\Omega \cdot cm^2$ at the dendrites, a uniform

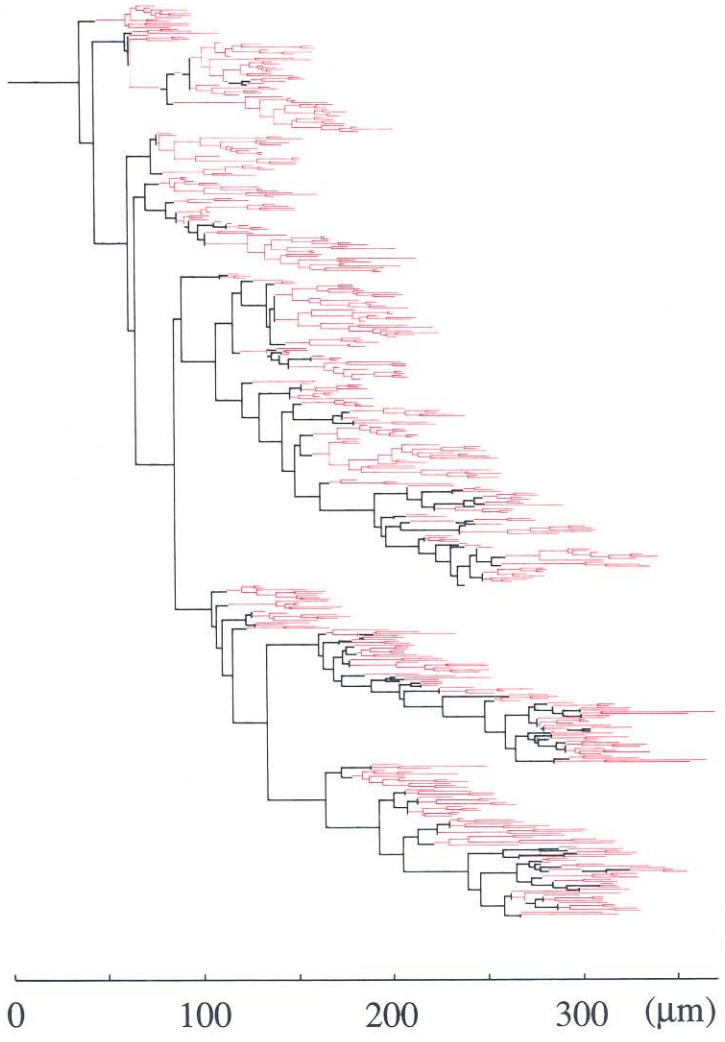

C_m of 1.64 μF/cm^2 and R_i of 250 $\Omega \cdot$ cm. These values yielded an input resistance, R_N, of 12.9 MΩ and a system time constant, τ_0, of 46 msec, both matching the corresponding experimental values. Morphological measurements of the cell in Figure 1 showed that the total length of dendritic branchlets bearing spines is 10,230 μm. These branchlets are marked by the red lines of Figure 2, which demonstrates Sholl diagram of the cell in Figure 1. The density of spines on the spiny branchlets has been reported to range between 10 and 14 per 1 μm dendritic length (Harris and Stevens 1988a,b); we estimated the total number of spines in the modeled tree to be 100,000, each with an area of 1 μm^2 (Harris and Stevens 1988a,b). The total soma–dendritic surface area (including spines) of the modeled neuron was 149,500 μm^2.

In most of the simulations spines were incorporated into the model globally, rather than by representing each spine as a separate segment, since the latter would be computationally very slow. It can be shown that, for plausible values of R_m, R_i, and C_m, when current flows *from the dendrite into the spine*, the membrane area of the spine can be incorporated into the membrane of the parent dendrite (Fig. 3A). The reason for this is that for this direction of current flow, the spine base and the spine head membranes are essentially isopotential (Jack *et al.* 1975; Rall and Rinzel 1973; Segev and Rall 1988). This approximation is valid when cable parameters such as R_N, τ_0, and the average cable length of the dendrites, L_{av}, are estimated from the model. It does not hold when the *voltage response* of the p.f. input impinging onto the spine head is of interest. In this case spines receiving synaptic input were represented in full (Fig. 3B).

To incorporate the spines globally into the model we modified the method suggested by Holmes (1989). In this method the original dimensions of the parent dendrite are preserved and the membrane area of the spines is effectively incorporated into the dendritic membrane by changing the values of R_m and C_m. When both spines and parent dendrite have the same specific membrane properties (R_m and C_m), the transformed values are:

$$R'_m = R_m/F \qquad \text{and} \qquad C'_m = C_m F$$

and

$$F = \frac{\text{area}_{\text{dend}} + \text{area}_{\text{spines}}}{\text{area}_{\text{dend}}} \tag{2.1}$$

where $\text{area}_{\text{dend}}$ is the area of the parent dendrite without the spines and $\text{area}_{\text{spines}}$ is the membrane area of the spines at that dendritic segment. Note that this transformation preserves the time constant of the original spiny dendrite.

The present study focuses on the effect of the conductance change induced by the p.f. input on the cable properties of the PC. In this case the effective membrane resistivity at the spine heads receiving the input ($R_{m,\text{actspines}}$) is reduced as compared to the membrane resistivity of

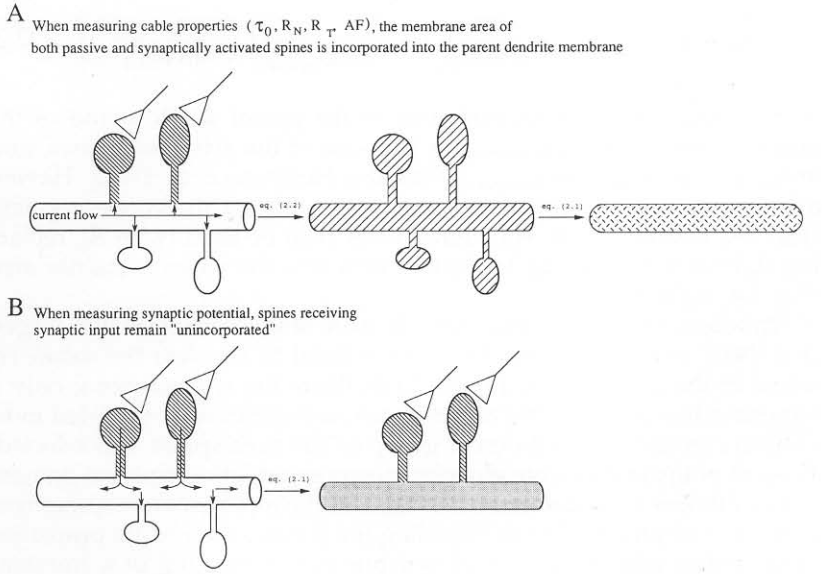

Figure 3: Schematic representation of the method used to globally incorporate dendritic spines into the membrane of the parent dendrite. (A) The case where the current flows from the dendrite into the spines (arrows in left schematic). (B) The case where current flows from the spines into the dendrite. In (A), equation 2.2 is first used to calculate an effective R_m value for the whole segment (middle schematic); then equation 2.1 is utilized for calculating new specific values for the membrane of the parent branch to effectively incorporate the spine area into the parent dendrite area. In (B), spines receiving synaptic input remain unincorporated, whereas passive spines are incorporated into the parent dendrite membrane as in (A).

the nonactivated spines and of the parent segment ($R_{m,\text{rest}}$). Assuming that the input can be approximated by a *steady-state* conductance change (see below), the effective time constant of the spiny segment (dendrite plus spines) is between the time constant of the dendritic membrane ($R_{m,\text{rest}} \cdot C_m$) and that of the activated spines membrane ($R_{m,\text{actspines}} \cdot C_m$). Now the first step in utilizing equation 2.1 is to find a single R_m^* value for the whole dendritic segment (parent dendrite plus all spines) such that ($R_m^* \cdot C_m$) approximates the effective time constant of the original (nonhomogeneous) segment. Our calculations show that for an electrically short spiny segment, R_m^* is the reciprocal of the sum of the specific

conductances of the two membrane types, weighted by their relative area:

$$R_m^* = 1/\left[\left(\frac{1}{R_{m,\text{rest}}}\right)\left(\frac{\text{area}_{\text{rest}}}{\text{area}_{\text{total}}}\right) + \left(\frac{1}{R_{m,\text{actspines}}}\right)\left(\frac{\text{area}_{\text{actspines}}}{\text{area}_{\text{total}}}\right)\right] \quad (2.2)$$

where $\text{area}_{\text{rest}}$ is the membrane area of the parent dendrite and of the nonactivated spines, $\text{area}_{\text{actspines}}$ is the area of the activated spines, and $\text{area}_{\text{total}} = (\text{area}_{\text{rest}} + \text{area}_{\text{actspines}})$ (see also Fleshman *et al.* 1988). Having a single R_m^* value as calculated in equation 2.2 for the whole segment (Fig. 3A, middle panel), equation 2.1 can then be used (with R_m^* replacing R_m) for incorporating the spines area into the parent dendrite area (Fig. 3A, right panel).

Transient (compartmental) models were studied using SPICE (Segev *et al.* 1985, 1989). These models were utilized to simulate the *voltage response* of the parallel fiber input. To facilitate the computations, only a representative group of 200 *randomly* selected spines were modeled individually. In each run a different group of 200 such spines was selected. The rest of the spines were globally incorporated into the parent branchlets membrane as discussed above. Each of the representative spines was simulated by an R-C circuit, modeling the passive membrane properties of the spine, and an additional synaptic path consisting of a transient conductance change, $g_{\text{syn}}(t)$, in series with a synaptic battery, E_{syn}. This compartment was connected to the parent dendrite by an axial resistance, representing the longitudinal resistivity of the spine neck (Segev and Rall 1988). The representative spines were activated synchronously at a high frequency, ω, such that $\omega = N \cdot \theta/200$ where N is the number of p.f.s and θ is the original (low) firing frequency of the p.f.s. For example, if each of the $N = 100,000$ p.f.s is activated at $\theta = 2$ Hz (200,000 inputs/sec), then each of the 200 representative spines is activated once every msec ($\omega = 1000$ Hz), thus preserving the total number of inputs per unit time. The validity of this approximation was examined by increasing the number of representative spines to 400 and decreasing ω by a factor of 2. These changes resulted in only minor differences in both the cable properties and the membrane voltage produced at the modeled cell. Also, the input resistance, R_N, as calculated using SPICE matched the analytical results of the cable models (see below). These control tests have led us to conclude that for the range of input frequencies tested, because of the large number of inputs impinging on the tree, the results of the present study are essentially independent of the exact timing of the input and/or the location of the activated spines, provided that the total conductance change per unit time is preserved.

Intuitively, a dendritic tree which is bombarded by a massive transient synaptic input must experience approximately a steady conductance change (Rall 1962). This *effective* conductance change, g_{steady}, can then be utilized in steady-state (segmental) cable models to compute analytically the impact of the synaptic activity on the cable properties of the cell.

For each transient synaptic input, $g_{syn}(t)$, activated at a frequency θ, the effective steady conductance change is

$$g_{steady} = \theta \int_0^\infty g_{syn}(t)\, dt \tag{2.3}$$

When 200 representative spines were used, ω replaced θ in equation 2.3. In that case, each of these spines has an effective R_m value,

$$R_{m,actspines} = \frac{area_{spine}}{g_{steady} + g_{rest}} \tag{2.4}$$

where $area_{spine}$ is the membrane area of the spine and $g_{rest} = (area_{spine}/R_{m,rest})$ is the resting conductance of the spine membrane (without the synaptic input). This $R_{m,actspines}$ value, over an area, $area_{actspines} = 200\ \mu m^2$ (200 spines), was utilized in equation 2.2 to calculate the effective R_m^* value of the spiny branchlets, with $area_{total}$ being the total membrane area of *all spiny branchlets* plus spines. In this way the total synaptic conductance was equally distributed over the whole membrane surface of the spiny branchlets.

In our computations, $g_{syn}(t)$ was modeled with an "alpha function,"

$$g_{syn}(t) = g_{max}(t/t_{peak}) \exp\{1 - (t/t_{peak})\} \tag{2.5}$$

where g_{max} is the peak synaptic conductance change and t_{peak} is the rise time. For the alpha function the integral in equation 2.3 is

$$\int_0^\infty g_{syn}(t)\, dt = g_{max} t_{peak} \exp(1) \tag{2.6}$$

With the values used in the present study ($g_{max} = 0.4$ nS; $t_{peak} = 0.3$ msec), this integral is 0.33 nS·msec. For $\theta = 2$ Hz ($\omega = 1000$ Hz) we get from equation 2.3 that $g_{steady} = 0.33$ nS. Thus, with a spine area of 1 μm^2 and $R_{m,rest}$ of 110,000 $\Omega \cdot cm^2$, equation 2.4 implies that the effective membrane resistivity of each of the activated spines is as small as 30 $\Omega \cdot cm^2$. Utilizing equation 2.2 with this value (with $area_{rest} = 144,538\ \mu m^2$ and $area_{actspines} = 200\ \mu m^2$), the effective R_m^* at the *spiny branchlets* was 18,140 $\Omega \cdot cm^2$ (rather than 110,000 $\Omega \cdot cm^2$), suggesting that the activation of the p.f.s have a marked effect on the cable properties of the PC.

Having R_m and R_i values for the tree, the algorithm developed by Rall (1959) was implemented to analytically calculate the effect of p.f. activation on the soma input resistance (R_N), the average input resistance at the terminals (R_T), the average cable length of the dendrites (L_{av}), and the average voltage attenuation factor from the dendritic tips into the soma ($AF_{T \to S}$); see also Nitzan *et al.* (1990). The modifications needed to include nonuniform R_m distribution is given in Fleshman *et al.* (1988). The system time constant (τ_0) was computed by "peeling" the voltage response to a brief current pulse produced by the corresponding compartmental model (Rall 1969).

The values for the unitary synaptic conductance change are based on the patch-clamp studies by Hirano and Hagiwara (1988) and Llano *et al.* (1991). The value for g_{max} was estimated from the minimal peak of the current produced by the p.f. input whereas the value for t_{peak} was estimated from the experimental rise time (measured at 22°C) corrected to 37°C, assuming a Q_{10} of 3.

3 Results

The voltage responses of the modeled PC to the p.f. input are shown in Figure 4 for an input frequency (θ) of 0.5 Hz (Fig. 4A) and 5 Hz (Fig. 4B). In each of these panels the continuous lines depict the voltage response at an arbitrarily chosen spine head (top trace), at the base of this spine (middle trace), and at the soma (lower trace). The bottom panels (C and D) show the corresponding input into each of the 200 representative spines (ω = 250 Hz in Fig. 4C and 2500 Hz in Fig. 4D). Dashed lines in A and B are the voltage responses at the corresponding sites when a steady state conductance change (g_{steady}), as defined in equation 2.3, is imposed on each of the 200 representative spines. This steady input shown by the dashed line in the corresponding lower panels is 0.08 nS in Figure 4C and 0.8 nS in Figure 4D (in the latter case the dashed line is masked by the heavy line). Unlike the case of relatively low input frequency (Fig. 4C) where each transient input is seen individually, at high frequency (Fig. 4D) the temporal summation of individual inputs resulted in the heavy line.

The figure demonstrates that already at a low firing rate of 0.5 Hz (Fig. 4A) the p.f. input produces a peak depolarization of approximately 15 mV at the spine head, 12 mV at the spine base, and 8 mV at the soma. At 5 Hz (Fig. 4B), the maximal depolarization at the spine head is 45 mV, 42 mV at the spine base, and 30 mV at the soma. An important difference in the voltage produced by the two input frequencies is in the *rate* of the voltage buildup. At a low frequency (Fig. 4A), the depolarization reaches a steady-state value after more than 100 msec whereas at high frequency (Fig. 4B) the steady-state value is reached after approximately 50 msec (see Discussion).

Figure 4 also shows that the steady-state approximation (dashed lines) faithfully reproduces the voltage response of the cell already at the low firing rate of 0.5 Hz (Fig. 4A). The agreement between the results of the transient input and the steady-state input implies that, indeed, the depolarization along the tree is essentially a function of $\omega \cdot g_{max} \cdot t_{peak}$ (equations 2.3 and 2.5). Thus, ω, g_{max}, and t_{peak} are interchangeable. Another point to note is that, unlike the case of a localized synaptic input where a significant voltage attenuation is expected, when a distributed input is activated the depolarization along the soma–dendritic surface is rather uniform (compare the voltage at the spine head and at the soma).

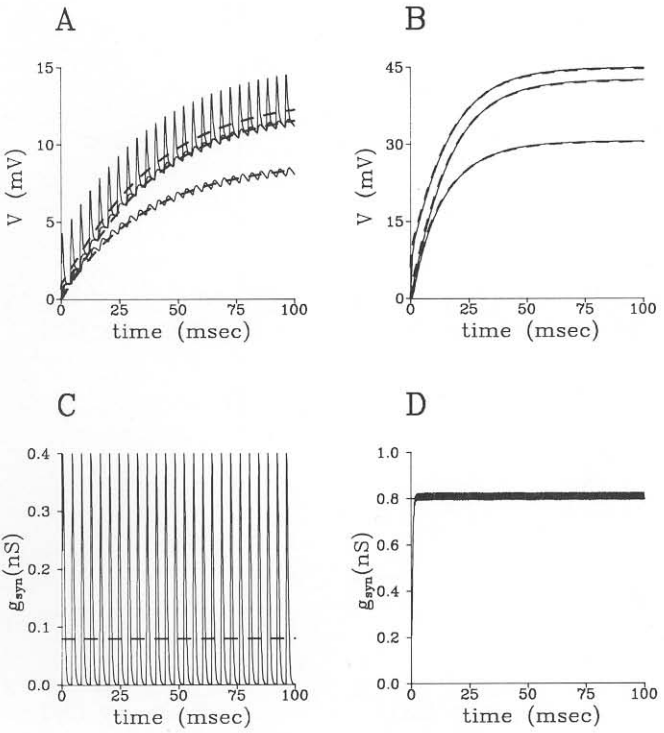

Figure 4: Depolarization produced by background activity of the parallel fibers. (A,C), $\theta = 0.5$ Hz; (B,C), $\theta = 5$ Hz. Bottom frames show the conductance input into each of the 200 representative spines modeled in full. Each of these spines receives transient conductance input at a frequency $\omega = \theta\,(100{,}000/200) = 500\theta$; individual inputs are clearly seen at the low firing rate (C). At the higher frequency (D) the transient synaptic conductance changes are summed-up to produce the heavy line. Dashed line in (C) and (D) [masked by the heavy line in (D)] shows the corresponding steady-state conductance change as calculated from equation 2.3. Upper panels (A and B) show the resultant depolarization at the head of one of the activated spines (upper curve), at its base (middle curve) and at the soma (lower curve). Dashed lines show the results when a steady-state conductance change is used. Note the excellent agreement between the results using transient inputs and the results obtained with a steady-state conductance change.

How do the different cable properties of the cell and the soma depolarization depend on the frequency of the p.f. input? Figure 5A shows

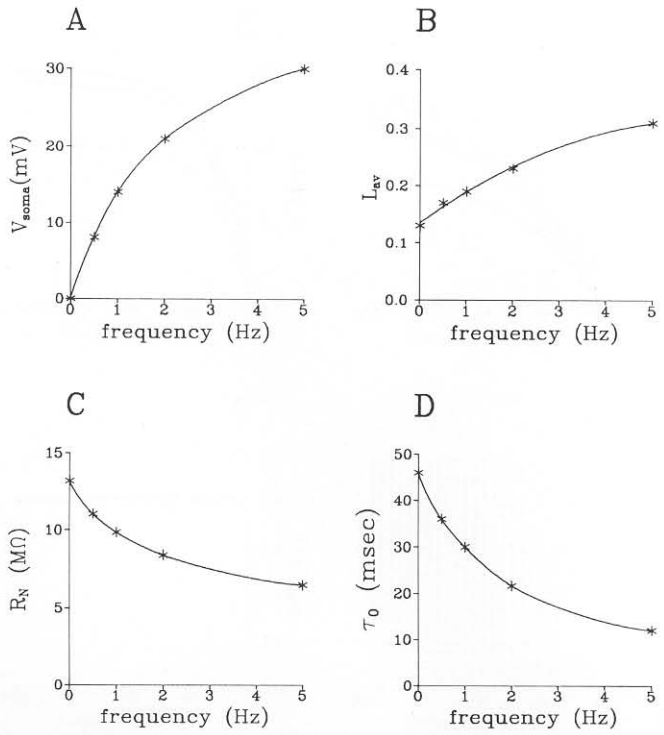

Figure 5: The cable properties of the PC critically depend on the input frequency (θ) of the parallel fibers. The graphs show this dependence on θ for (A) the depolarization produced at the PC soma, (B) the average electrotonic length of PC dendrites, (C) the soma input resistance, and (D), the system line constant. The points in (A) were calculated using SPICE; the points in (B–D) were calculated analytically. These changes will influence the efficacy of the p.f. input.

that the depolarization at the soma changes steeply at low frequencies and tends to saturate at higher frequencies. The saturated value of somatic depolarization induced by the p.f. input was found to be $\frac{2}{3}E_{syn}$, namely 40 mV for the parameters chosen in the present study.

The effect of the p.f. input frequency on the average cable length (L_{av}) of the dendritic tree is shown in Figure 5B. Due to the high R_m value at rest (at $\theta = 0$ Hz) L_{av} is 0.13. The tree is electrically "stretched" into $L_{av} = 0.31$ (a factor of 2.4) at 5 Hz. At this range of frequencies the input resistance at the soma (Fig. 5C) is decreased from 12.9 MΩ at

0 Hz to 6.5 MΩ at 5 Hz (50%), whereas the average input resistance at the terminal tips (R_T) is reduced by only 20% (from 104 to 83 MΩ, not shown). The system time constant (Fig. 5D) is the most sensitive parameter; it is reduced from 46 to 12.1 msec (a factor of 3.8, see also Rall 1962). This implies that, at 5 Hz, the effective membrane conductance is four times larger than the membrane conductance at 0 Hz. Another parameter that was calculated (not shown) is the average steady state attenuation factor ($AF_{T\to S}$) from the terminal tips to the soma. This parameter is increased from 8.8 (at 0 Hz) to 28 (at 5 Hz), a factor of 3.2. For the explicit relation between R_T and $AF_{T\to S}$ (see Rall and Rinzel 1973).

We conclude that the background activity of the p.f.s significantly changes the cable properties of the PC dendrites with the following relative sensitivity: $\tau_0 > AF_{T\to S} > L_{av} > R_N > R_T$. The somatic depolarization resulting from p.f.s activation rises steeply as a function of the input frequency. Already at relatively low firing frequency of 5 Hz it reaches 3/4 of the maximal depolarization that the p.f.s can produce at the PC's soma (Fig. 5A). This depolarization develops rather smoothly with a rate that increases as the input frequency increases.

4 Discussion

The present study demonstrates that the background activity of the parallel fibers has a dramatic effect on the functional properties of cerebellar Purkinje cells. Already at a low firing rate of a few Hz, the membrane conductance of the PC significantly increases. As a result, both the system time constant, τ_0, and the input resistance, R_N, decrease by several fold, whereas the electronic length, L_{av}, and the voltage attenuation factor, $AF_{T\to S}$ (not shown) increase (Fig. 5B–D). This background activity is expected to significantly depolarize the PC (Fig. 4A & B and Fig. 5A). The effect of the background activity on the cable properties of the cell strongly depends on the time-integral of the synaptic conductance change and on the frequency of the background activity (equation 2.3).

The same general results hold also for other neurons from the mammalian CNS receiving a large number of synaptic contacts, each of which may be activated spontaneously at a frequency of a few spikes/sec. Indeed, similar conclusions have been recently reached by Bernander *et al.* (1991) who modeled the effect of background activity on the cable properties of a reconstructed layer V pyramidal cell in the visual cortex. We therefore suggest that the effective cable properties and the "resting potential" of these neurons *in the behaving animal* are different from those measured in the slice preparation or in anesthetized animals (Holmes and Woody 1989; Abbott 1991; Amit and Tsodyks 1992).

The results of the present study have several interesting implications for the integrative capabilities of central neurons. The massive background activity (and the corresponding increase in the membrane con-

ductance) implies that single p.f. inputs essentially loose their functional meaning and only the activation of a large number of p.f.s will significantly displace the membrane potential. It should be noted, however, that other more efficient individual inputs (which may also contact a different dendritic region and do not participate in the background activity) can have a marked effect on the input/output characteristics of the PC. An example is the powerful climbing fiber input which forms as many as 200 synaptic contacts on the soma and main dendrite of the Purkinje cell. When activated, the whole dendritic tree and soma are strongly depolarized; this produces a short burst of high-frequency firing at the PC axon (Llinás and Walton 1990).

As demonstrated in Figure 5A, the soma depolarization (the excitatory synaptic current reaching the soma) is a nonlinear function of the input firing rate. The higher the frequency of the background activity, the larger the number of excitatory synapses that need to be recruited to depolarize the cell by a given amount. This is in contrast to the presently used neuron network models, where the current input into a modeled "cell" is assumed to be linearly related to the input firing rate. The saturation of the soma depolarization at relatively low firing rates (Fig. 5A) implies a narrow dynamical range for the detection of changes in p.f. input frequency.

Figure 4A and B show that for any given input frequency, several tens of milliseconds are required for the voltage to reach a steady-state value. Therefore, changes in the frequency of the p.f. input will be "detected" only if the change lasts for a relatively long period. Furthermore, because of the change in τ_0, the time course of the voltage change is a function of the input frequency. The higher the input frequency, the faster the build-up of the potential toward its steady value. Hence, at higher background frequencies, more synapses are required to shift the membrane potential by a given amount, but the time course of this shift is faster. For example, suppose that the frequency of the background activity of the p.f.s is 1 Hz (100 synapses/msec); the resulting depolarization (relative to 0 Hz) is 13 mV (Fig. 4A). Increasing the frequency to 2 Hz (an additional 100 synapses/msec) will further depolarize the soma by 8 mV, provided that the frequency change lasts at least 50 msec (about 2.5 times τ_0 corresponding to 2 Hz; Fig. 4D). These dynamic alternations in the depolarization of the PC soma will modulate the cell firing rate.

Inhibitory inputs onto the PC originate primarily from the *stellate cells* (dendritic inhibition) and from the *basket cells* (mainly somatic inhibition). Since our model has a very leaky soma (low somatic R_m), the basket cell input is essentially built-in to the model. The number of stellate cells that contact a single PC is much smaller than the number of p.f.s. It is expected, therefore, that the *background* activity onto the PC will be dominated by the activity of the p.f.s. Our preliminary simulations suggest that the inhibition induced by the stellate cells can act only locally,

at a given dendritic region, and have only a minor effect on the somatic membrane potential produced by the p.f. activity.

Finally, it has been clearly shown that the PC's dendrites are endowed with a variety of voltage-sensitive channels (Llinás and Sugimori 1980a,b). In response to synaptic inputs, these channels produce both subthreshold nonlinearities as well as full blown dendritic spikes. The effect of these nonlinearities on the results of the present report will be explored in a future study.

Acknowledgments

This work was supported by a grant from the Office of Naval Research and a grant from the Israeli Academy of Sciences. We thank our colleague Shaul Hochstein for critical comments on this work.

References

Abbott, L. F. 1991. Realistic synaptic input for model neural networks. *Network* (in press).

Amit, D. J., and Tsodyks, M. V. (1992). Effective neurons and attractor neural networks in cortical environment. *Network* (in press).

Barrett, J. N., and Crill, W. E. 1974. Specific membrane properties of cat motoneurones. *J. Physiol. (London)* **293**, 301–324.

Bernander, O., Douglas, R. J., Martin, K. A. C., and Koch, C. 1992. Synaptic background activity determines spatio-temporal integration in single pyramidal cells. *Proc. Natl. Acad. Sci. U.S.A.* **88**, 11569–11573.

Brown, T. H., Fricke, R. A., and Perkel, D. H. 1981. Passive electrical constants in three classes of hippocampal neurons. *J. Neurophysiol.* **46**, 812–827.

Crapel, F., and Penit-Soria, J. 1986. Inward rectification and low threshold calcium conductance in rat cerebellar Purkinje cells. *J. Physiol. (London)* **372**, 1–23.

Fleshman, J. W., Segev, I., and Burke, R. E. 1988. Electrotonic architecture of type-identified α motoneurons in the cat spinal cord. *J. Neurophysiol.* **60**, 60–85.

Harris, K. M., and Stevens, J. K. 1988a. Dendritic spines of rat cerebellar Purkinje cells: Serial electron microscopy with reference to their biophysical characteristics. *J. Neurosci.* **12**, 455–469.

Harris, K. M., and Stevens, J. K. 1988b. Study of dendritic spines by serial electron microscopy and three-dimensional reconstruction. *Neurol. Neurobiol.* **37**, 179–199.

Hirano, T., and Hagiwara, S. 1988. Synaptic transmission between rat cerebellar granule and Purkinje cells in dissociated cell culture: Effects of excitatory-amino acid transmitter antagonists. *Proc. Natl. Acad. Sci. U.S.A.* **85**, 934–938.

Holmes, W. R. 1989. The role of dendritic diameter in maximizing the effectiveness of synaptic inputs. *Brain Res.* **478**, 127–137.

Holmes, W. R., and Woody, C. D. 1989. Effect of uniform and non-uniform synaptic "activation-distribution" on the cable properties of modeled cortical pyramidal cells. *Brain Res.* **505**, 12–22.

Jack, J. J. B., Noble, D., and Tsien, R. W. 1975. *Electrical Current Flow in Excitable Cells*. Oxford University Press, UK.

Jack, J. J. B., and Redman, S. J. 1971a. The propagation of transient potentials in some linear cable structures. *J. Physiol. (London)* **215**, 283–320.

Jack, J. J. B., and Redman, S. J. 1971b. An electrical description of the motoneuron, and its application to the analysis of synaptic potentials. *J. Physiol. (London)* **215**, 321–352.

Llano, I., Marty, A., Armstrong, C. M., and Konnerth, A. 1991. Synaptic and agonist-induced excitatory current of Purkinje cells in rat cerebellar slices. *J. Physiol. (London)* **431**, 183–213.

Llinás, R. R., and Sugimori, M. 1980a. Electrophysiological properties of in vitro Purkinje cell somata in mammalian cerebellar slices. *J. Physiol. (London)* **305**, 171–195.

Llinás, R. R., and Sugimori, M. 1980b. Electrophysiological properties of in vitro Purkinje cell dendrites in mammalian cerebellar slices. *J. Physiol. (London)* **305**, 197–213.

Llinás, R. R., and Walton, K. D. 1990. Cerebellum. In *The Synaptic Organization of the Brain*, G. M. Shepherd, ed., pp. 214–245. Oxford University Press, Oxford.

Nitzan, R., Segev, I., and Yarom, Y. 1990. Voltage behavior along irregular dendritic structure of morphologically and physiologically characterized vagal motoneurones in the guinea pig. *J. Neurophysiol.* **63**, 333–346.

Rall, W. 1959. Branching dendritic trees and motoneuron membrane resistivity. *Exp. Neurol.* **1**, 491–527.

Rall, W. 1962. Theory of physiological properties of dendrites. *Ann. NY Acad. Sci.* **96**, 1071–1092.

Rall, W. 1964. Theoretical significance of dendritic trees for neuronal input-output relations. In *Neural Theory and Modeling*, R. Reiss, ed., pp. 73–97. Stanford University Press, Stanford.

Rall, W. 1967. Distinguishing theoretical synaptic potentials computed for different soma-dendritic distributions of synaptic input. *J. Neurophysiol.* **30**, 1138–1168.

Rall, W. 1969. Time constants and electronic length of membrane cylinders in neurons. *Biophys. J.* **9**, 1483–1168.

Rall, W. 1977. Core conductor theory and cable properties of neurons. In *Handbook of Physiology*, Vol. 1, Pt. 1. *The Nervous System*, E. R. Kandel, ed., pp. 39–97. Americal Physiology Society, Bethesda, MD.

Rall, W., and Rinzel, J. 1973. Branch input resistance and steady attenuation for input to one branch of a dendritic neuron model. *Biophys. J.* **13**, 648–688.

Rapp, M. 1990. The passive cable properties and the effect of dendritic spines on the integrative properties of Purkinje cells. M.Sc. Thesis, submitted to the Hebrew University, Jerusalem.

Segev, I., and Rall, W. 1988. Computational study of an excitable dendritic spine. *J. Neurophysiol.* **60**, 499–523.

Segev, I., Fleshman, J. W., Miller, J. P., and Bunow, B. 1985. Modeling the electrical properties of anatomically complex neurons using a network analysis program: Passive membrane. *Biol. Cyber.* **53**, 27–40.

Segev, I., Fleshman, J. W., and Burke, R. E. 1989. Compartmental models of complex neurons. In *Methods in Neuronal Modeling: From Synapses to Networks*, C. Koch and I. Segev, eds., pp. 171–194. Bradford Books, Cambridge, MA.

Segev, I., Rapp, M., Manor, Y., and Yarom, Y. 1992. Analog and digital processing in single nerve cells: Dendritic integration and axonal propagation. In *Single Neuron Computation*, T. McKenna, J. Davis, and S. F. Zornetzer, eds. Academic Press, Orlando, FL (in press).

Stratford, K., Mason, A., Larkman, A., Major, G., and Jack, J. 1989. The modelling of pyramidal neurons in the visual cortex. In *The Computing Neuron*, R. Durbin, C. Miall, and G. Mitchison, eds., pp. 296–321. Addison-Wesley, Wokingham, England.

Received 23 July 1991; accepted 12 December 1991.